PHYSICAL REVIEW E, VOLUME 64, 010803(R)

Interfacial and topological measurements of bicontinuous polymer morphologies

Hiroshi Jinnai,[1,*] Takashi Kajihara,[1] Hideyuki Watashiba,[1] Yukihiro Nishikawa,[2] and Richard J. Spontak[3,†]
[1]*Department of Polymer Science and Engineering, Kyoto Institute of Technology, Kyoto 606-8585, Japan*
[2]*Structural Biochemistry, The Institute of Physical and Chemical Research (RIKEN), 1-1-1 Kouto, Mikaduki, Sayo, Hyogo 679-5148, Japan*
[3]*Department of Chemical Engineering and Department of Materials Science & Engineering, North Carolina State University, Raleigh, North Carolina 27695*
(Received 2 January 2001; published 28 June 2001)

Bicontinuous morphologies are ubiquitous in nature and occur at various length scales. Topological features of two such morphologies arising in an ordered block copolymer at equilibrium and a polymer blend during spinodal decomposition are measured from three-dimensional images. Interfacial curvature, coordination number, and interjunction distance distributions exhibit remarkable similarity in these systems, despite vastly different length scales. A channel coordination of 3 is dominant in both morphologies, and topological measurements such as the Euler-Poincaré characteristic and genus are reported.

DOI: 10.1103/PhysRevE.64.010803 PACS number(s): 61.41.+e

Interpenetrating network morphologies exhibiting bicontinuity occur naturally at different length scales in numerous systems of biological and physical interest. Detailed characterization of such morphologies, which may appear grossly similar, is often hindered by their topological complexity. Block copolymers and their blends, for instance, exhibit several bicontinuous nanostructures, including the gyroid [1], perforated lamellar [2], sponge [3] and microemulsion [4] morphologies. This is due principally to immiscibility between the dissimilar constituent sequences [5,6]. A subtle balance between interfacial tension and molecular packing frustration dictates the local shape of the interface, which ultimately determines the global morphology [7,8]. These bicontinuous polymer nanostructures are widely believed to share common topological features with other examples of soft-condensed matter that are also capable of spontaneous molecular self-organization (e.g., surfactant and lipid systems) [9,10]. At larger length scales, transient bicontinuous morphologies measuring on the order of micrometers develop during the spinodal decomposition (SD) of phase-separating liquid mixtures. In this case, the onset of morphology formation reflects thermodynamic instability, whereas structural evolution is again driven by an overall reduction in interfacial area [11,12]. An example of a bicontinuous morphology measuring on the order of millimeters is trabecular bone [13].

Direct measurements of local and global structural parameters are requisite for the complete characterization of complex bicontinuous morphologies. Mean (H) and Gaussian (K) interfacial curvatures constitute structural parameters that together describe the local shape of the interface. As predicted [7] and confirmed experimentally [8], the averages *and* distributions of these parameters are essential for a thorough understanding of the molecular origin and stability of bicontinuous nanostructures. Quantitation of the time evolution of interfacial curvature distributions can likewise elucidate the mechanism responsible for interfacial development during phase separation [12]. In contrast, topological measurements of bicontinuous morphologies would provide global structural details, such as the number of intersecting channels per junction (the coordination number, N_j) and the distance between adjacent junctions (the interjunction distance, D_j). Such measurements yield another important, but experimentally unexplored, set of structural parameters by which to characterize and compare, in quantitative fashion, complex morphologies.

The value of N_j is particularly important with regard to the assignment of bicontinuous morphologies, since it can be used to differentiate between closely related morphologies, such as the gyroid (G, $N_j=3$) and diamond (D, $N_j=4$). Additional parameters that further serve to classify topologies on the basis of the number of existing junctions and channels are the Euler-Poincaré characteristic (χ) and genus (g) [10]. Prior attempts to measure the interfacial and topological characteristics of complex nanostructures in reciprocal space by scattering methods have provided little insight into the local and global *shape* and *connectivity* of complex block copolymer nanostructures. Such information can, however, be gleaned directly from real-space measurements of three-dimensional (3D) images [8]. In this work, we measure the interfacial curvatures and several topological features of two bicontinuous polymer morphologies, one in an ordered block copolymer and the other in a phase-separated polymer blend, from 3D images obtained by transmission electron microtomography (TEMT) and laser-scanning confocal microscopy (LSCM), respectively.

A poly(styrene-*b*-isoprene-*b*-styrene) (SIS) triblock copolymer was synthesized via living anionic polymerization. Its number-average molecular weight, $\overline{M}_n$, and polydispersity index were 8.3×10^4 and 1.09, respectively, and its composition was 32 vol% styrene (S). Specimens for TEMT were produced according to the protocol described earlier [3,14]. The SD polymer blend was composed of deuterated polybutadiene (DPB) and polybutadiene (PB). The $\overline{M}_n$ values and polydispersity indices were 8.9×10^4 and 1.07, re-

*Electronic address: hjinnai@ipc.kit.ac.jp
†Electronic address: rich_spontak@ncsu.edu

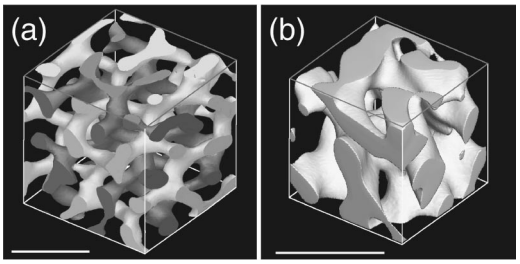

FIG. 1. Three-dimensional images of bicontinuous morphologies in two composition-matched polymer systems: (a) the *G* nanostructure in a microphase-ordered block copolymer (bar=74 nm) and (b) the SD morphology in an off-critical polymer blend (bar $=20.4\ \mu$m). In (a), the nonintersecting light and dark channels correspond to the minority microphase, while the majority microphase is transparent. In (b), the minority phase is shown, while the majority phase is transparent. Corresponding skeletal networks generated after channel thinning are displayed in (c) and (d), respectively.

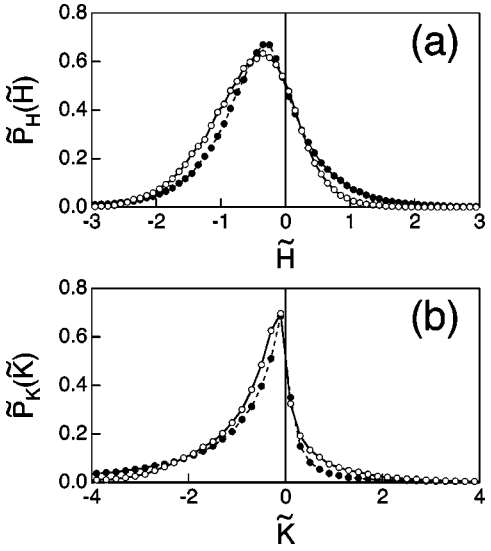

FIG. 2. Scaled probability densities (a) $\tilde{P}_H(\tilde{H})$ and (b) $\tilde{P}_K(\tilde{K})$ measured from the bicontinuous block copolymer $G(\bigcirc)$ and polymer blend SD ($\bullet$) morphologies.

spectively, for DPB and 12.7×10^4 and 1.12, respectively, for DPB. The DPB blend exhibited an upper critical solution temperature at a composition of 46 vol% DPB. A 37.8/62.2 v/v DPB-PB blend was homogenized and then annealed at 40 °C for 2943 min, which induced late-stage SD. Volumetric images of the phase-separated blend were acquired by LSCM, as detailed elsewhere [12]. Two-dimensional (2D) slices of each 3D reconstruction were subjected to conventional image processing, and then binarized using an appropriate threshold. The trajectory of the isointensity line corresponding to the threshold value was used to identify the interface, which was represented in 3D by first stacking the 2D images and then applying the marching cube algorithm [15] to model the interface as contiguous triangles [16]. Application of the sectioning and fitting algorithm [17] to each resultant image furnished values of H and K at randomly selected points on each interface. As described elsewhere [8], numerous points were sampled to generate statistically meaningful distributions of H and K.

Figure 1(a) shows the reconstructed 3D image of the triblock copolymer nanostructure, which consists of two nonintersecting channel networks within a continuous matrix. (The light and dark channels evident in this figure both represent the S microphase, but are shaded differently to demonstrate that the two channel networks do not intersect.) For the sake of clarity, the volume-filling I microphase is transparent. According to the reconstruction, this nanostructure is 33 vol% S, in good agreement with the calculated composition. Previous crystallographic analysis [8] reveals that this nanostructure is consistent with the *G* morphology and possesses a characteristic length scale (Λ) of 74 nm. Displayed in Fig. 1(b) is the reconstructed 3D image of the bicontinuous SD morphology of the DPB-PB blend. In this case, the channels correspond to the DPB-rich phase, the volume fraction of which is measured to be 0.37. As in Fig. 1(a), the volume-filling matrix (PB) is rendered transparent to facilitate visualization. Note that the two polymer systems possess similar composition to facilitate comparison. Unlike the copolymer nanostructure, the DPB-PB blend morphology consists of a two-channel bicontinuous network in which $\Lambda=20.4\ \mu$m, as discerned from the position of the intensity maximum of the calculated structure factor.

The local shape of the interface in each of the 3D images provided in Fig. 1 can be described by a joint probability density of interfacial curvatures, $P(H,K)$. Quantities characterizing the local geometry of a bicontinuous interface include H and K, where $H=(\kappa_1+\kappa_2)/2$ and $K=\kappa_1\kappa_2$ (κ_1 and κ_2 denote the principal curvatures at a given point on the interface). From $P(H,K)$, the probability densities of the mean and Gaussian curvatures, $P_H(H)$ and $P_K(K)$, respectively, can be calculated [12]. The curvature is arbitrarily chosen to be positive if the center of the osculating circle resides within the I microphase of the copolymer or the PB phase of the polymer blend. To facilitate comparison, $P_H(H)$ and $P_K(K)$ have been scaled with respect to the interfacial area per unit volume (Σ) in the following fashion:

$$\tilde{P}_H(\tilde{H})=P_H(H)\Sigma,\quad \tilde{P}_K(\tilde{K})=P_K(K)\Sigma^2. \tag{1}$$

Here, $\tilde{H}=H\Sigma^{-1}$ and $\tilde{K}=K\Sigma^{-2}$, with Σ equal to 0.070 nm^{-1} for the copolymer and 0.136 μm^{-1} for the blend. The $\tilde{P}_H(\tilde{H})$ and $\tilde{P}_K(\tilde{K})$ determined from the two bicontinuous morphologies shown in Fig. 1 are displayed in Fig. 2 and exhibit surprising similarity. In Fig. 2(a), $\tilde{P}_H(\tilde{H})$ for each morphology exhibits a broad maximum at $\tilde{H}<0$, in which case the area-averaged mean curvature is non-zero. Most of $P_K(\tilde{K})$ for each morphology in Fig. 2(b) resides at $\tilde{K}<0$, indicating that each interface is mainly hyperbolic. Despite the minor differences evident in Fig. 2, it is intriguing that the interfacial curvature distributions of these two bicontinuous morphologies differing in characteristic size by a factor of over 300 are so strikingly similar.

A skeletonizing algorithm based on the one proposed by Yasue *et al.* [18] has been developed [19], which (i) system-

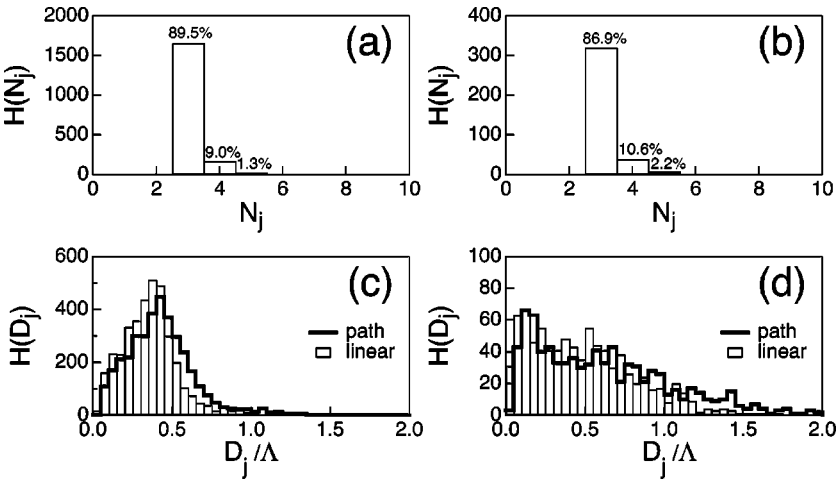

FIG. 3. Histograms of the coordination number (N_j) for (a) the G nanostructure and (b) the SD morphology. In both cases, the dominant N_j is 3. Corresponding histograms of the normalized interjunction distance (D_j/Λ) are provided in (c) and (d), respectively. The thick line denotes D_j evaluated along the network path, whereas the thin line represents the linear distance between junctions.

atically excludes junctions attached to the edge planes of the experimental volume element from statistical treatment, and (ii) applies the Euclidean distance transformation [20] to ensure that each skeletonized network strand locates at the center of its precursor channel. Cursory examination of Fig. 1 suggests that the skeletal network of the G nanostructure in Fig. 1(c) is more regularly arranged than that of the SD morphology in Fig. 1(d). The average number of junctions per crystallographic unit cell (N_{cell}) for the nanostructure is 11, which is in fair agreement with $N_{cell}=15$ measured from a computer-generated constant-thickness (CT) model surface of the G morphology based on the Schoen G surface (the composition of this surface is 33/67 v/v to equal that of the SIS copolymer [8]). Note that the mathematically predicted value of N_{cell} for the CT surface is 16. The discrepancy in N_{cell} between the G morphology and composition-matched CT surface is attributed to the presence of defects in the grains or along the grain boundaries of the G morphology (the CT Schoen G surface is free from such defects). A comparison of the measured and predicted values of N_{cell} for the CT surface demonstrates the level of accuracy in the 3D channel-thinning protocol employed here. In contrast to the G copolymer nanostructure, N_{cell} discerned from the SD blend morphology is only 1.9, thereby confirming that the junctions are more densely packed in the nanostructure. Distributions of the coordination number (N_j) are displayed in Fig. 3(a) for the G nanostructure and in Fig. 3(b) for the SD morphology. Both morphologies possess, for the most part, three branches at each junction. Higher coordination numbers account for less than circa 13% of each N_j distribution. Since the requisite N_j for the G morphology is 3, the statistical result that $N_j \sim 3$ provides further experimental evidence that the copolymer morphology is G, which is consistent with previous (but limited) observations [14].

Shown in Fig. 3 are distributions of scaled D_j for the copolymer [Fig. 3(c)] and polymer blend [Fig. 3(d)]. Two measurements of D_j are provided in each figure: one represents the shortest distance between junctions (*linear* distance) and the other corresponds to the distance along the skeletal network (*path* distance). Although common features between the G and SD morphologies are evident in the interfacial curvature distributions (Fig. 2) and the coordination number distributions [Figs. 3(a) and 3(b)], this is clearly not the case with respect to D_j. According to the data presented in Fig. 3(b), the G morphology exhibits maxima in D_j at 0.40 Λ (linear) and 0.45 Λ (path). These values are in favorable agreement with those derived from the CT model surface (0.40 Λ). The SD morphology of the polymer blend, however, exhibits a shoulderlike broad maximum in D_j at 0.5–0.7 Λ (linear and path distances). The data displayed in Fig. 3(d) also reveal that, unlike the G nanostructure, the SD morphology consists of a large population of junctions separated by surprisingly short distances in the range of 0.1–0.2 Λ.

The Euler-Poincaré characteristic (χ) can be estimated from the total number of junctions (N) and the total number of branches (B) through $\chi=2N-B$ [21]. Here, $B=\Sigma_{i=0}^{N} N_{j,i}$, where $N_{j,i}$ denotes the coordination number at the ith junction. Values of χ per unit cell are -12.1 for the G nanostructure and -3.3 for the SD morphology. Corresponding values of the genus (g), another topological measure characterizing the complexity of a network and related to χ through $g=1-\chi/2$, are 7.1 and 2.6, respectively. To put this results in perspective, a surface with genus g is topologically equivalent to a sphere with g handles. For comparison, the CT model surface yields $\chi=-14.7$ (-16.0) and $g=8.4$ (9.0) (values in parentheses are mathematically predicted quantities). These values agree well with the corresponding values discerned for the G morphology in Fig. 1(a). Differences in χ and g between the G nanostructure and the composition-matched CT Schoen G surface are again ascribed to defects and grain boundaries. According to the Gauss-Bonnet theorem of differential geometry, χ is related to the Gaussian curvature by $2\pi\chi=\int K da=\langle K\rangle S$, where da denotes the area element of the surface and S is the interface area, if the surface is closed. From this theorem, we estimate χ to be -11.0 for the G nanostructure and -4.3 for the SD morphology (and -15.0 for the Schoen G surface). Since these values are reasonably close to those derived from the skeletonization analysis, the Gauss-Bonnet theorem appears to be applicable to these two bicontinuous morphologies, which can therefore be considered as closed surfaces.

In summary, topological parameters such as N_j and D_j have been measured *directly* in two bicontinuous polymer

morphologies, the characteristic size scales of which differ by a factor of more than two orders of magnitude. The interfacial area per unit volume is experimentally ascertained for each morphology, as is the interfacial area per copolymer molecule within the G nanostructure (3.1 nm^2/molecule). Interfacial curvature distributions characterize local morphological features and appear strikingly similar, suggesting that the two morphologies consist of small, comparably shaped interfacial ''patches.'' The global topologies of the two morphologies reveal how the interfacial patches are connected. In both morphologies, $N_j \sim 3$, which is anticipated for the G nanostructure, but not for the SD morphology. In contrast, normalized D_j distributions are strongly morphology-dependent. The maximum D_j measured for the G morphology is found to be in good quantitative agreement with that expected from the Schoen G surface, whereas the SD morphology possesses a broad distribution of interjunction distances. Experimental measurements of the Euler-Poincaré characteristic and genus corresponding to each morphology are provided as an additional set of topological parameters to facilitate comparison of these morphologies. Topologically speaking, we conclude that the G nanostructure of the block copolymer constitutes a more complex network than the late-stage SD morphology of the polymer blend.

This study has been supported by the Ministry of Education, Science, Sports and Culture, Japan (Grants-in-Aid Nos. 12750799 and 13031057) and the U.S. Department of Energy under Contract No. FG02-99ER14991. We are indebted to S.D. Smith for the block copolymer and D.A. Agard for technical assistance.

[1] D. A. Hajduk *et al.*, Macromolecules **27**, 4063 (1994); M. F. Schulz *et al.*, Phys. Rev. Lett. **73**, 86 (1994); F. S. Bates and G. H. Fredrickson, Phys. Today **52**, 32 (1999).

[2] D. A. Hajduk *et al.*, Macromolecules **30**, 3788 (1997); R. J. Spontak and P. Alexandridis, Curr. Opin. Colloid Interface Sci. **4**, 140 (1999).

[3] J. H. Laurer *et al.*, Langmuir **13**, 2250 (1997).

[4] F. S. Bates *et al.*, Phys. Rev. Lett. **79**, 849 (1997); H. S. Jeon *et al.*, Macromolecules **31**, 3340 (1998); D. Schwahn *et al.*, Phys. Rev. Lett. **82**, 5056 (1999).

[5] E. L. Thomas *et al.*, Nature (London) **334**, 598 (1988).

[6] I. W. Hamley, *The Physics of Block Copolymers* (Oxford University Press, New York, 1998).

[7] M. W. Matsen and F. S. Bates, Macromolecules **29**, 7641 (1996).

[8] H. Jinnai *et al.*, Phys. Rev. Lett. **84**, 518 (2000).

[9] S. M. Gruner, J. Phys. Chem. **93**, 7562 (1989).

[10] S. T. Hyde *et al.*, *The Language of Shape* (Elsevier Science B.V., Amsterdam, 1997).

[11] H. Jinnai *et al.*, Phys. Rev. Lett. **78**, 2248 (1997).

[12] H. Jinnai *et al.*, Langmuir **16**, 4380 (2000).

[13] M. Ito *et al.*, Bone **23**, 163 (1998).

[14] J. H. Laurer *et al.*, Macromolecules **30**, 3938 (1997); R. J. Spontak *et al.*, *ibid.* **29**, 4494 (1996).

[15] W. E. Lorensen and H. E. Cline, Comput. Graph. **21**, 163 (1987).

[16] Y. Nishikawa *et al.*, Langmuir **14**, 1242 (1998).

[17] Y. Nishikawa *et al.*, Langmuir **17**, 3254 (2001).

[18] M. Yasue *et al.*, IEICE Trans. **J79**, 1664 (1996).

[19] Y. Nishikwa, H. Jinnai, and H. Hasegawa, Kobunshi Ronbunshu **58**, 13 (2001).

[20] T. Saito and J. Toriwaki, Pattern Recogn. **27**, 1551 (1994).

[21] S. T. Hyde and S. Ramsden, in *Discrete Mathematical Chemistry*, edited by P. Hansen *et al.* (American Mathematical Society, DIMACS, Providence, 2000), Vol. 51, p. 203.